1723

Calculation of Water Displacement by Gas in Development of Aquifer Storage

K. H. COATS*
J. G. RICHARDSON
MEMBERS AIME

ESSO PRODUCTION RESEARCH CO.
HOUSTON, TEX.

1723

ABSTRACT

During the initial growth of a gas bubble in an aquifer storage reservoir the injected gas tends to override the water. The resulting low displacement efficiency and high rate of gas travel down-structure make it difficult to maintain water-free production. This paper illustrates the use of two-dimensional, two-phase calculations to simulate this gas-water displacement. Calculations were performed for a stratified aquifer and for several homogeneous sands differing in permeability, porosity and thickness. Results are discussed and compared with performance predictions obtained from the simpler Buckley-Leverett and Dietz formulas. This comparison indicates the necessity for the two-dimensional calculations in realistically simulating the gravity override of the water by injected gas.

INTRODUCTION

In recent years natural gas has been stored near markets in aquifers where insufficient storage capacity is available in depleted fields. Operators of these aquifer storage reservoirs have encountered technical problems relating to the gas-water displacement accompanying initial growth of the gas bubble. Injected gas tends to override the water, with a resultant low displacement efficiency and high rate of gas travel down-structure toward spill points. Low displacement efficiency makes if difficult to sustain water-free gas production. Sometimes the fingering of gas down-structure may be so pronounced that the injection rate must be severely curtailed, which excessively lengthens the time required for bubble growth.

This paper is concerned with estimating — for given aquifer characteristics and fluid properties — the displacement efficiency, rate of gas movement down-structure and rate of gravity drainage of water behind the gas front. Several published articles relate to simulative capability necessary to handle this problem. The Dietz formula[1] and Buckley-Leverett[2] method have some applicability to the problem; Woods and Comer[3] reported one-dimensional, radial calculations which accounted for the two-phase flow of gas and water. Most recent research directed toward understanding aquifer behavior in relation to gas storage has concentrated on single-phase flow in aquifer.[4] Douglas, Peaceman and Rachford[5] presented a method for calculating multi-dimensional two-phase flow in reservoirs; their method has been applied in work reported by Nielsen and Tek,[6] Blair and Peaceman[7] and Goddin.[8] Refs. 5 and 7 show comparisons between experimental data and calculations similar to those employed here.

One purpose of this paper is to illustrate the use of two-dimensional, two-phase flow calculations in simulating the difficult problem of water displacement by gas in a vertical cross-section. The pronounced fluid density and viscosity differences combine with the disparity in horizontal and vertical dimensions of the cross-section to pose one of the more difficult problems in reservoir simulation. The calculations described account for capillary and gravity forces, relative permeability and reservoir heterogeneity. An example reservoir is described and calculated results are presented for a variety of injection rates and values of permeability, reservoir thickness and dip angle. A second purpose is to compare the two-dimensional calculations with results obtained from the Buckley-Leverett and Dietz formulas. For this reason most calculations were performed for a simplified example reservoir to which the latter techniques might reasonably be applied. However, the computer program employed applies equally well to cases involving arbitrary spatial variations of permeability, porosity, reservoir thickness and dip angle.

Original manuscript received in Society of Petroleum Engineers office Nov. 3, 1966. Revised manuscript of SPE 1723 received March 23, 1967. Paper was presented at Pennsylvania State U. 25th Annual Technical Conference on Petroleum Production held in Philadelphia, Pa., Oct. 19, 1966.

*Currently associate professor of petroleum engineering at The U. of Texas, Austin, Tex.

[1]References given at end of paper.

BASIC EQUATIONS

The well-known, basic equations governing two-phase flow in porous media are (1) Darcy's law for each fluid phase, (2) the continuity equation expressing conservation of mass and (3) the definition of capillary pressure. These three equations are combined as shown in the Appendix to give Eqs. 1. Gas and water are treated as incompressible.

$$\nabla \cdot \left(k \frac{k_{rw}}{\mu_w} \nabla \Phi_w\right) + B_w q_w = -\phi S' \frac{\partial \Phi_w}{\partial t} + \phi S' \frac{\partial \Phi_g}{\partial t} \quad \ldots (1a)$$

$$\nabla \cdot \left(k \frac{k_{rg}}{\mu_g} \nabla \Phi_g\right) + B_g q_g = \phi S' \frac{\partial \Phi_w}{\partial t} - \phi S' \frac{\partial \Phi_g}{\partial t} \quad \ldots (1b)$$

Eq. 2 gives the critical rate[9] as a function of formation and fluid properties,

$$q_{gc} = 7.82 \times 10^{-9} \frac{kA}{B_g} \frac{\rho_w - \rho_g}{\mu_w - \mu_g} \sin \alpha_d \text{ MMCF/D}, \quad \ldots (2)$$

where A is cross-sectional area perpendicular to the direction of flow.

This formula is derived by balancing viscous and gravitational forces about a small finger of gas extending down-structure into the water parallel to the bedding plane. [Eq. 2 and the following Dietz Eq. 3 may be written with μ_w/k_{rw}, μ_g/k_{rg} replacing μ_w and μ_g. However, this replacement requires choice of the gas saturation (e.g., frontal saturation or average saturation behind front) at which k_{rg} is to be evaluated. That question deserves extensive consideration and has in fact been the subject of several previous papers. For the sake of simplicity, and to avoid lengthy discussion of a subject somewhat apart from the purpose of this paper, k_{rg} is excluded from Eqs. 2 and 3. The critical rate given by Eq. 2 is therefore used here only as a reference rate; it is not viewed as a rate at which unstable fingering of gas necessarily begins. Rates above the critical rate given by Eq. 2 may, in fact, yield a favorable mobility ratio at the displacement front.]

Sustained gas injection above the critical rate is undesirable, since the displacement of water will be inefficient and the gas may finger unstably down-structure at a high rate. The critical rate thus serves as a useful guide or reference rate in establishing the gas injection rate during bubble growth. Where the critical rate is far lower than the injection rate, gravity segregation plays little role in preventing a rapid rate of gas travel down-structure.

For injection rates below the critical, the Dietz formula (Eq. 3) gives the angle between the bedding plane and the gas-water interface as a function of rate and formation and fluid properties.[1]

$$\tan \theta = \tan \alpha_d - 128 \times 10^{6} \frac{q_g B_g}{kA} \frac{\mu_w - \mu_g}{(\rho_w - \rho_g)\cos \alpha_d} \quad \ldots (3)$$

To evaluate the utility of this formula, the predicted angle is compared with results calculated from Eqs. 1.

One of the reservoir scaling groups derived by Rapoport and Leas[10] for incompressible, two-phase flow is the ratio of viscous to gravitational forces $\frac{q\mu_w/Lk}{L\Delta\rho}$. Since injection rate q and permeability k appear only as the ratio q/k, their effects on reservoir performance can be considered as the single effect of the ratio q/k.

DISPLACEMENT STUDIES

SCOPE

Two-dimensional calculations employing Eq. 1 were performed to simulate the growth of a gas bubble in a slightly dipping aquifer. The example aquifer or reservoir was represented by a homogeneous, vertical cross-section described below. Calculations were performed for various values of injection rate, permeability, reservoir thickness and dip angle. A severely stratified case was also treated to illustrate the effect of heterogeneity. The two-dimensional calculations were performed on a vertical cross-section to describe the gas overriding the water. This overriding tendency has a great effect on the efficiency with which water is displaced.

DESCRIPTION OF EXAMPLE RESERVOIR

The example reservoir treated here is patterned roughly after the Mt. Simon aquifer storage field.[11] Fig. 1 illustrates the homogeneous vertical slice or cross-section, 3,000 ft long and 100 ft thick with a 3° dip angle. Gas injection rate is based on a width of 7,500 ft. The injection rate and fluid and rock properties for the reservoir (Table 1) constitute the base case (Case 1) for the calculations. Relative permeability and capillary pressure curves listed in Table 1 were averaged from data on a number of permeable Eocene sandstone core samples.

TABLE 1 — DATA FOR EXAMPLE RESERVOIR, BASE CASE

Water density	62.4 lb/cu ft
Gas density	3 lb/cu ft
Water viscosity	1 cp
Gas viscosity	0.013 cp
Water formation volume factor	1 res. bbl/STB
Gas formation volume factor	2.55 res. bbl/Mcf
Permeability	200 md
Porosity	0.15
Reservoir length	3,000 ft
Reservoir width	7,500 ft
Reservoir thickness	100 ft
Dip angle, sine	0.05
Initial saturation	100 percent water
Injection rate	5 MMcf/D
2-D grid	$N_x=30, N_z=10$
Critical rate q_{gc}	1.38 MMcf/D

Capillary Pressure-Relative Permeability Data

Water Saturation (fraction)	Capillary Pressure (psi)	Water Relative Permeability (fraction)	Gas Relative Permeability (fraction)
.22	15.0	.0	1.0
.23	8.8	.00018	.977
.25	6.2	.00045	.925
.3	3.57	.0013	.802
.35	2.76	.00215	.683
.4	2.45	.003	.573
.45	2.16	.006	.466
.5	1.86	.012	.372
.55	1.57	.022	.287
.6	1.29	.04	.211
.65	1.0	.065	.152
.7	.71	.099	.106
.75	.42	.146	.069
.8	.09	.202	.043
.85	−.22	.285	.023
.9	−.56	.418	.008
.95	−.91	.675	.002
.99	−1.3	.932	.0
1.0	−1.5	1.0	.0

Table 2 gives data and results for all seven cases calculated. Cases 2 through 7 involve variations in permeability, reservoir thickness, dip angle and gas injection rate. For each case in Table 2, data not reported are identical with those given in Table 1. Table 2 also includes the ratio of injection rate to critical rate for each case.

PROCEDURE

Eqs. 1 were solved simultaneously employing ADIP.[5] The cross-section was represented by a 30 × 10 grid, yielding a block 100 ft long by 10 ft thick (30 × 5 grid in cases involving 50-ft thickness).

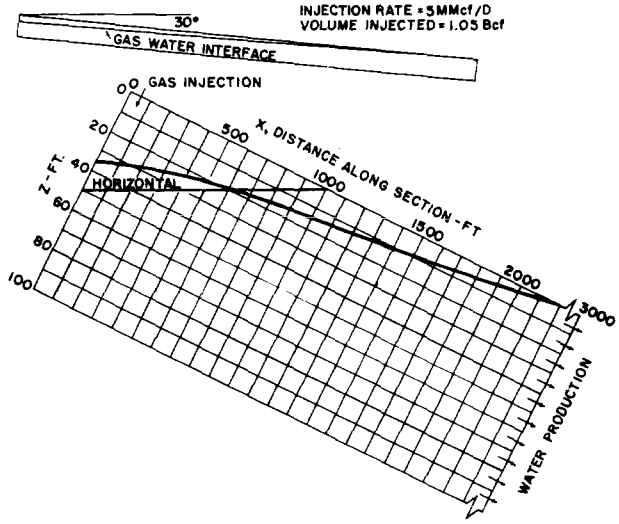

FIG. 1 — CALCULATED POSITION OF GAS-WATER INTERFACE, BASE CASE.

Gas was injected into the top corner block of the reservoir (Fig. 1). Water was produced from all 10 blocks through the thickness at the downdip end of the section. Iterations at each time step were continued until the incremental material balance satisfied a closure tolerance. About eight iterations per time step were required. Cumulative material balance, defined as total gas in place divided by total gas actually injected, was generally less than 0.5 percent, always less than 1 percent in error. Time steps were limited so that the maximum block saturation change was less than 10 percent in one time step.

As an example of computer time requirements, using 57 time steps to simulate injection at 1 MMcf/D for 1,050 days (Case 2) required 16.84 minutes of IBM 7044 time ($200 per hour).

BASE CASE RESULTS

Data for the base case are given in Table 1. The injection rate is 5 MMcf/D into a 200-md formation 100 ft thick and 7,500 ft wide. Fig. 1 shows the calculated position of the gas-water interface after 210 days, or cumulative injection of 1.05 Bcf. The 5 MMcf/D rate is 3.62 times the critical rate and results in a severe gas override, as shown in the scale representation of the cross-section; the tongue of gas reaches over

TABLE 2 — DATA AND RESULTS FOR CASES 1 THROUGH 7

Case	Permeability (md)	Sine of Dip Angle	Thickness (ft)	Injection Rate (MMcf/D)	Cumulative Injection (Bcf)	Injection Rate/ Critical Rate	Displacement Efficiency (percent)	Distance of Gas Travel Down-Structure (ft)
1	200	.05	100	5	1.05	3.62	37.2	2,100
2	200	.05	100	1	1.05	.725	46.3	1,300
3	200	.25	100	5	1.05	.725	46.0	800
4	200	.05	100	2.5	1.05	1.81	43.3	1,800
4	200	.05	100	2.5	.525	1.81	39.4	1,100
5	200	.05	50	2.5	.525	3.62	33.5	1,600
6	Table 3	.05	50	2.5	.525	–	9.35	2,500
7	158	.05	50	2.5	.525	4.6	32.0	1,700

2,100 ft down-structure. The displacement efficiency, defined as the percentage of the water initially in place that is displaced from the region invaded by gas, is 37.2 percent (since relative permeability to water is 0 at a water saturation of 22 percent (Table 1), the maximum possible displacement efficiency is 78 percent). Fig. 2 shows depth-averaged gas saturation vs distance along the cross-section. Fig. 3 shows the rate of gas travel down-structure. The gas front travels 800 ft in 60 days and continues to move linearly with time.

COMPARISON WITH BUCKLEY-LEVERETT RESULTS

The Buckley-Leverett technique was applied to the base-case data of Table 1 to calculate saturation vs distance after 210 days of injection. Fig. 4 shows that the Buckley-Leverett and 2-D results are in poor agreement; the Buckley-Leverett technique gives a gas movement down-structure of only 700 ft compared with the 2,100 ft predicted by the 2-D method.

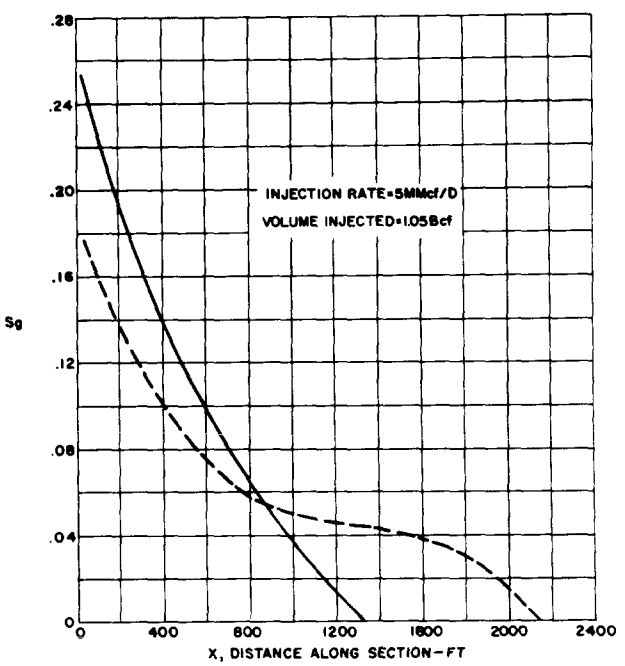

FIG. 2 — DEPTH-AVERAGED GAS SATURATION PROFILE, BASE CASE.

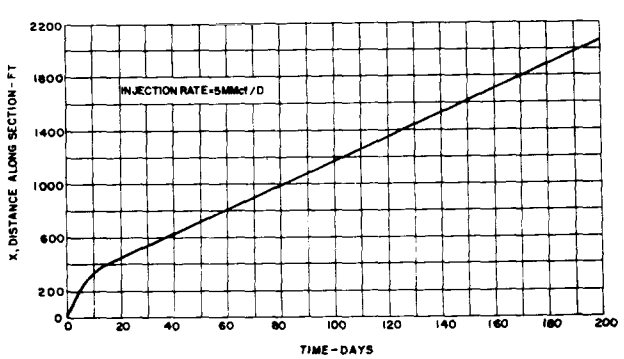

FIG. 3 — RATE OF GAS MOVEMENT DOWN-STRUCTURE, BASE CASE.

Fig. 5 shows equally poor agreement between Buckley-Leverett and 2-D results for an injection rate less than the critical rate (Case 2, Table 2). The primary reason for this poor agreement is the inability of the Buckley-Leverett method to account for the two-dimensional nature of the displacement (i.e., for the pronounced override of the water by the gas). The lack of applicability of the Buckley-Leverett results indicates the need for 2-D or 3-D calculations in simulating gravity override of water by injected gas.

COMPARISON OF 2-D RESULTS WITH DIETZ EQUATION

Two-dimensional calculations were performed for an injection rate less than the critical rate to compare the inclination of the gas-water interface with the inclination yielded by the Dietz Eq. 3. Fig. 6 shows the position of the gas-water interface given by two-dimensional calculations simulating 1,050 days of injection at 1 MMcf/D (Case 2, Table 2). Insertion of the Case 2 data into Eq. 3 yields tan $\theta = 0.0142$. In Fig. 6, the line drawn corresponding to that angle corresponds to a 100 percent displacement of mobile water, a displacement efficiency of 78 percent. The figure shows that the Dietz angle provides a good approximation to the inclination of the interface over the flat portion. However, the Dietz equation predicts only the angle, not the position of the interface. Positioning of the interface requires that the average

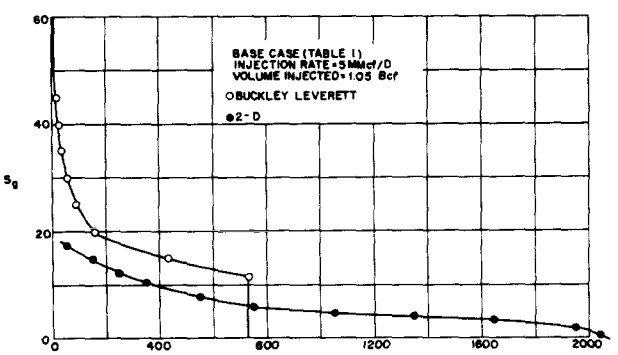

FIG. 4 — COMPARISON OF SATURATION PROFILES CALCULATED BY BUCKLEY-LEVERETT AND 2-D METHODS, BASE CASE.

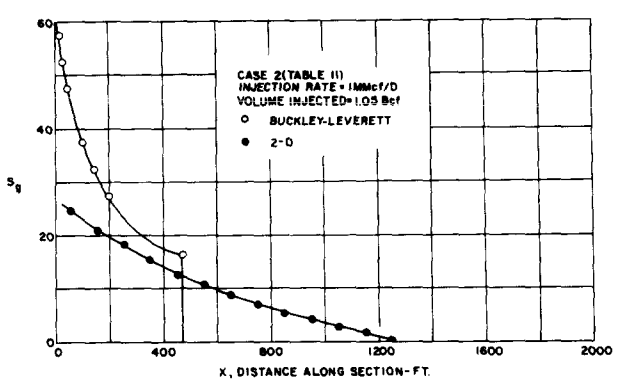

FIG. 5 — COMPARISON OF SATURATION PROFILES CALCULATED BY BUCKLEY-LEVERETT AND 2-D METHODS, CASE 2.

displacement efficiency behind the front be known, and determination of this efficiency requires 2-D calculations.

EFFECTS OF PERMEABILITY, DIP ANGLE AND THICKNESS

The 2-D results for Case 2 show how permeability affects the gas-water displacement. This case is identical with the base case except that injection rate is 1 MMcf/D, less than critical. Injection rate and permeability affect reservoir performance only through the ratio q/k, as previously discussed. Therefore, Case 2 results are identical with those for the case of a 5 MMcf/D rate of injection into a 1,000-md formation. Thus, comparison of results from Cases 1 and 2 shows how a five-fold larger permeability affects the displacement.

Fig. 6 shows the position of the gas-water interface after injection of 1.05 Bcf. Comparison with Fig. 1 shows that the higher permeability results in a more nearly horizontal interface, lesser extent of gas travel down-structure and higher displacement efficiency. For the 1,000-md permeability, the gas traveled only 1,300 ft down-structure compared with 2,100 ft in the 200-md case. The displacement efficiency for 1,000 md was 46.3 percent, compared with 37.2 percent for 200 md.

Case 3, as noted in Table 2, differs from the base case only in that the sine of the dip angle is increased from 0.05 to 0.25. As noted in Table 2, the higher dip angle reduces the gas travel down-structure after injection of 1.05 Bcf from 2,100 ft in the base case to 800 ft. The displacement efficiency rises from 37.2 to 46 percent. The injection rate of 5 MMcf/D for Case 3 is below critical (Table 2). These considerable effects of dip angle on rate of gas movement and displacement efficiency reflect the recognized desirability of locating steeply dipping structures for storage purposes.

Case 4 illustrates the effect of a 50 percent

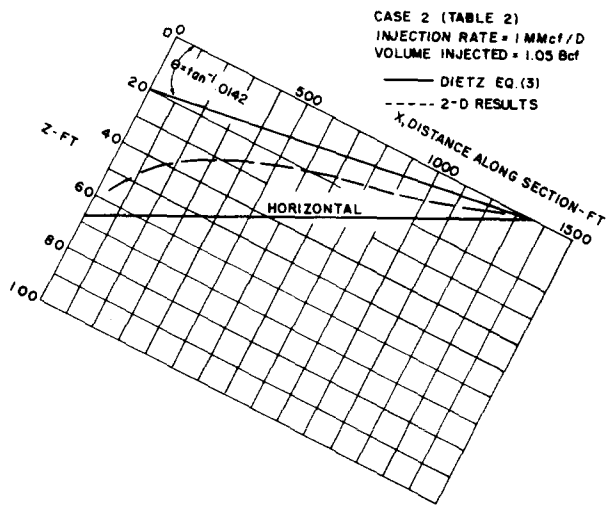

FIG. 6 — COMPARISON OF GAS-WATER INTERFACE POSITIONS OBTAINED FROM DIETZ EQUATION AND 2-D CALCULATIONS.

TABLE 3 — DESCRIPTION OF STRATIFIED AQUIFER, CASE 6

Layer (i)	Horizontal Permeability (md)	Vertical Permeability Between Layers i and $i+1$ (md)	Thickness (ft)
1	50	1.6	10
2	200	.727	10
3	20	.385	10
4	500	7.7	10
5	20	.0	10

Porosity = 0.15;
see Table 1 for other data.

reduction in injection rate to 2.5 MMcf/D. As noted in Table 2, displacement efficiency after injection of 1.05 Bcf rises from the base case 37.2 to 43.3 percent, and gas travel down-structure decreases from the 2,100-ft base case to 1,800 ft.

Case 5 shows how reservoir thickness affects displacement efficiency. Data for this case are identical with those for Case 4 except that reservoir thickness is reduced 50 percent to 50 ft. Displacement efficiency, after 0.525 Bcf injection, dropped from the 39.4 percent of Case 4 to 33.5 percent. Gas travel down-structure increased, reaching 1,600 ft as compared with 1,100 ft. These results indicate the desirability of thick sands in aquifer storage structures.

HETEROGENEOUS CASE

Cases 6 and 7 illustrate the effect of severe heterogeneity. Case 6 is a stratified formation with five layers varying from 20 to 500 md in permeability. The layer thicknesses and vertical permeabilities are given in Table 3. Case 7 is identical with Case 6 except that the reservoir is homogeneous with the same total millidarcy-feet product. Fig. 7 compares calculated positions of the gas-water interface after injection of 0.525 Bcf for the stratified and homogeneous cases. In the stratified formation a finger or wafer of gas in high-permeability Layer 4 reaches over 2,600 ft down-structure; in the homogeneous formation (equivalent

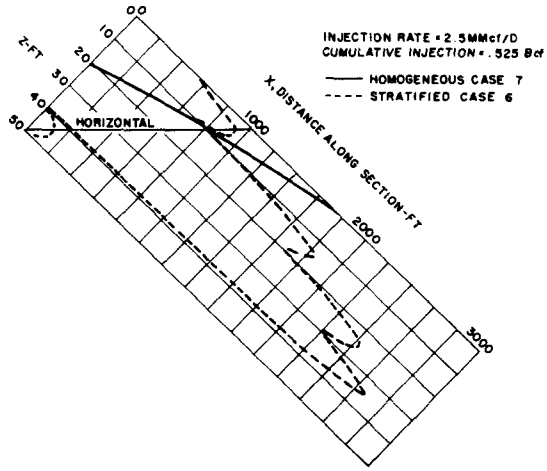

FIG. 7 — COMPARISON OF GAS-WATER INTERFACE POSITIONS IN STRATIFIED AND HOMOGENEOUS AQUIFERS.

Case 7), it reaches only 1,700 ft. Gas entered the tight Layers 1 and 3 in the stratified reservoir almost entirely by percolation upward from high-permeability Layers 2 and 4. The displacement efficiency in the stratified formation (Case 6) is only 9.35 percent, compared with 32 percent for the equivalent homogeneous formation (Case 7).

Fig. 8 shows calculated gas saturation contours for the stratified aquifer. The 5 percent saturation contour exhibits the same character as the interface contour of Fig. 7 in that it is further advanced in tight Layer 3 than in loose Layer 2. However, the 10 percent saturation contour exhibits the contrary behavior of further advancement in Layer 2 than in Layer 3. The reason for this situation is that the gas enters tight Layer 3 by percolating upward from Layer 4, and for small saturations (e.g., 5 percent or less) the low relative permeability to gas in Layer 3 retards further percolation upward to Layer 2. However, with higher gas saturations in Layer 3 (e.g., 10 percent or more), sufficiently high relative permeabilities to gas exist to allow significant flow upward to Layer 2, thus causing the character of the 10 percent saturation profile shown in Fig. 8.

The significant effect of heterogeneity in Case 6 shows the need for reservoir description. It is probably true that our ability to simulate reservoirs at the present time exceeds our ability to describe them. Considerable reliance on simulated performance is justified where sufficient core data, well tests and some history for matching purposes are available. However, simulation of performance can still be useful when little is known about the reservoir properties since calculations assuming a homogeneous sand will generally give a conservative estimate of the rate of gas travel down-structure and an upper limit on the displacement efficiency. (This statement holds for random arrangements of layers of differing permeability. However, it is not strictly true since one could easily design a stratification that would retard the gas fingering along the caprock and thereby increase displacement efficiency relative to the homogeneous case.) If calculations assuming a homogeneous sand indicate intolerably low displacement efficiencies and high rates of gas travel, perhaps past spill points, then they justify dismissal of the structure as a potential storage site.

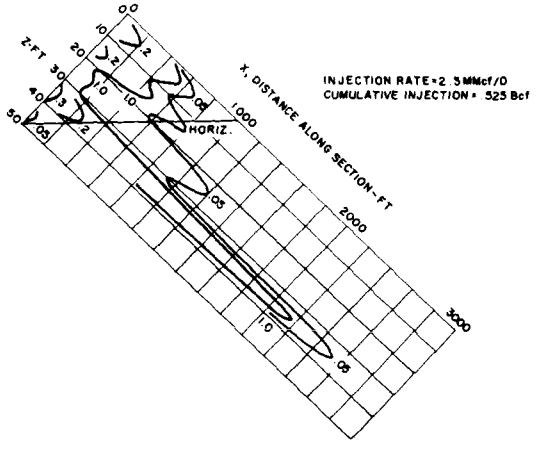

FIG. 8—CALCULATED GAS SATURATION CONTOURS IN STRATIFIED AQUIFER, CASE 6 (INJECTION RATE, 2.5 MMcf/D; CUMULATIVE INJECTION, 0.525 Bcf).

CONCLUSIONS

Based on the two-phase, two-dimensional calculations conducted in this study, and on comparisons of these with results of one-dimensional calculations, the following conclusions are reached.

1. Two-phase, two-dimensional calculations appear to be necessary for reliable estimates of displacement efficiency and rates of gas movement down-structure in aquifer storage projects.
2. Where possible, calculations should include the permeability distribution of the aquifer in question. Generally, when the sand is assumed to be homogeneous, displacement efficiencies are too high and rates of gas movement are too low.
3. For the type of displacement considered here, the Buckley-Leverett technique predicts displacement efficiencies that are too high and rates of gas movement that are too low.

NOMENCLATURE

B_g = gas formation volume factor, res. bbl/Mcf
B_w = water formation volume factor, res. bbl/surface bbl
h = depth, measured vertically downward, ft
k = absolute permeability, md
k_{rw}, k_{rg} = relative permeability to water and gas, respectively
N_x = number of grid points (blocks) in x direction
N_z = number of grid points in z direction
P_c = capillary pressure, psi
p = pressure, psi
q_{gc} = critical gas injection rate, MMcf/D
q_g(Eq.3) = gas injection rate, MMcf/D
q_g(Eq.4) = gas injection rate, Mcf/cu ft res./D
q_w = water injection rate, surface bbl/cu ft res./D
Q_w = water injection rate, surface B/D for block in grid
Q_g = gas injection rate, Mcf/D for block in grid
S_w = water saturation
$S' = dS_w/dP_c$
t = time, days
v = superficial velocity, cu ft/sq ft/D
α_d = formation dip angle
ϕ = porosity

ρ = density, lb/cu ft

μ = viscosity, cp

Φ = potential, $p - \frac{\rho}{144} h$

SUBSCRIPTS

w = water

g = gas

REFERENCES

1. Dietz, D. N.: "A Theoretical Approach to the Problem of Encroaching and By-Passing Edge Water", *Prec. Kan. Neder. Adad.*, Wetenshaffen, Series B-56 (1953) 83.
2. Buckley, S. E. and Leverett, M. C.: *Trans.*, AIME (1942) Vol. 146, 107.
3. Woods, E. G. and Comer, A. G.: "Saturation Distribution and Injection Pressure for a Radial Gas Storage Reservoir", *J. Pet. Tech.* (Dec., 1962) 1389-1393.
4. Katz. D. L. *et al.*: "Movement of Underground Water in Contact with Natural Gas", AGA Monograph on Project 31, New York (1963).
5. Douglas, J., Jr., Peaceman, D. W. and Rachford, H. H., Jr.: "A Method for Calculating Multi-Dimensional Immiscible Displacements", *Trans.*, AIME (1959) Vol. 216, 297-308.
6. Nielsen, R. L. and Tek, M. R.: "Evaluation of Scale-Up Laws for Two-Phase Flow through Porous Media", *Soc. Pet. Eng. J.* (June, 1963) 164-176.
7. Blair, P. M. and Peaceman, D. W.: "An Experimental Verification of a Two-Dimensional Technique for Computing Performance of Gas-Drive Reservoirs", *Soc. Pet. Eng. J.* (March, 1963) 19-27.
8. Goddin, C. S., Jr. *et al.*: "A Numerical Study of Waterflood Performance in a Stratified System With Crossflow", *J. Pet. Tech.* (June, 1966) 765-771.
9. Hill, S.: Genie Chemique, *Chem. Eng. Sci.*, I (6): 246 (1952).
10. Rapoport, L. A. and Leas, W. J.: "Properties of Linear Waterfloods", *Trans.*, AIME (1953) Vol. 198, 139-148.
11. Rzepczynski, W. M., Katz, D. L., Tek, M. R. and Coats, K. H.: "How the Mt. Simon Gas Storage Project Was Developed", *Oil and Gas J.* (June 19, 1961).

APPENDIX

3-D FLOW EQUATIONS

The basic equations governing incompressible, two-phase flow in porous media are the continuity or material balance equations for each phase,

$$-\nabla \cdot (v_w) + B_w q_w = \frac{\partial}{\partial t} \cdot (\emptyset S_w) \quad \ldots\ldots\ldots (4a)$$

$$-\nabla \cdot (v_g) + B_g q_g = \frac{\partial}{\partial t} (\emptyset S_g) \quad \ldots (4b)$$

Darcy's law relating superficial velocities to flow potential,

$$v_w = -k \frac{k_{rw}}{\mu_w} \nabla \Phi_w$$

$$v_g = -k \frac{k_{rg}}{\mu_g} \nabla \Phi_g \quad \ldots\ldots (5)$$

and the capillary pressure definition

$$P_c = p_g - p_w \quad \ldots\ldots\ldots (6)$$

Eq. 6, along with the definition of Φ,

$$\Phi_w = p_w - \frac{\rho_w}{144} h$$

$$\Phi_g = p_g - \frac{\rho_g}{144} h \quad \ldots\ldots (7)$$

allows expression of the saturation derivative $\frac{\partial S_w}{\partial t}$ in terms of the potentials,

$$\frac{\partial S_w}{\partial t} = S' \left[\frac{\partial \Phi_g}{\partial t} - \frac{\partial \Phi_w}{\partial t} \right] \quad \ldots (8)$$

Substitution of Eqs. 5 and 8 into Eqs. 4 yields two equations in the two dependent variables Φ_w and Φ_g,

$$\nabla \cdot \left(k \frac{k_{rw}}{\mu_w} \nabla \Phi_w\right) + B_w q_w = -\emptyset S' \frac{\partial \Phi_w}{\partial t} + \emptyset S' \frac{\partial \Phi_g}{\partial t} \quad \ldots (9a)$$

$$\nabla \cdot \left(k \frac{k_{rg}}{\mu_g} \nabla \Phi_g\right) + B_g q_g = \emptyset S' \frac{\partial \Phi_w}{\partial t} - \emptyset S' \frac{\partial \Phi_g}{\partial t} \quad \ldots (9b)$$

where $S' = dS_w/dP_c$. Multiplying Eqs. 9 by the block volume $\Delta x\, \Delta y\, \Delta z$, and writing derivations in difference form, yields

$$\Delta A_w \Delta \Phi_w + B_w Q_w = - G \Delta_t \Phi_w + G \Delta_t \Phi_g$$

$$\Delta A_g \Delta \Phi_g + B_g Q_g = G \Delta_t \Phi_w - G \Delta_t \Phi_g$$

where

$$\Delta A \Delta \Phi = \Delta_x AX \Delta_x \Phi + \Delta_y AY \Delta_y \Phi + \Delta_z AZ \Delta_z \Phi$$

$$\Delta_x AX \Delta_x \Phi = AX_{i+1/2,j,k} (\Phi_{i+1,j,k} - \Phi_{ijk}) - AX_{i-1/2,j,k} (\Phi_{ijk} - \Phi_{i-1,j,k})$$

$$AX_{i+1/2,j,k} = \left(k \frac{k_r}{\mu} \frac{\Delta y \Delta z}{\Delta x}\right)_{i+1/2,j,k}$$

$$G = \frac{PV\, S'}{\Delta t} = \frac{\emptyset \Delta x \Delta y \Delta z\, S'}{\Delta t}$$

$$\Delta_t \Phi = \Phi^{n+1}_{ijk} - \Phi^{n}_{ijk}$$

$$x = i\Delta x \quad y = j\Delta y \quad z = k\Delta z \quad t = n\Delta t$$

***